



A multiscale coupling method for the modeling of dynamics of solids with application to brittle cracks

Xiantao Li^{a,*,1}, Jerry Z. Yang^b, Weinan E^{c,2}

^a Department of Mathematics, Pennsylvania State University, University Park, PA 16802, USA

^b School of Mathematical Sciences, Rochester Institute of Technology, Rochester, NY 14623, USA

^c Department of Mathematics and Program in Applied and Computational Mathematics, Princeton University, Princeton, NJ 08544, USA

ARTICLE INFO

Article history:

Received 8 September 2009

Received in revised form 21 January 2010

Accepted 31 January 2010

Available online 10 February 2010

Keywords:

Molecular dynamics

Multiscale methods

Crystalline solids

ABSTRACT

We present a multiscale model for numerical simulations of dynamics of crystalline solids. The method combines the continuum nonlinear elasto-dynamics model, which models the stress waves and physical loading conditions, and molecular dynamics model, which provides the nonlinear constitutive relation and resolves the atomic structures near local defects. The coupling of the two models is achieved based on a general framework for multiscale modeling – the heterogeneous multiscale method (HMM). We derive an explicit coupling condition at the atomistic/continuum interface. Application to the dynamics of brittle cracks under various loading conditions is presented as test examples.

© 2010 Elsevier Inc. All rights reserved.

1. Introduction

Traditional continuum models of solids are based on empirical constitutive relations. Linear elasticity is a good example of such empirical models, in which the properties of material response is represented by very few parameters, e.g. the elastic moduli. However, in many cases the accuracy of these empirical constitutive relations is insufficient. This is generally the case when strong defects such as cracks are present in the material. In this case, it is crucial to model at least some aspects of the atomic processes near the defects, even if our interest is only on the overall mechanical response of the material. Therefore, it is of great practical interest to develop multiscale models, which incorporate a microscopic description with the continuum model.

In recent years, there has been a growing amount of effort on developing multiscale models that combine atomistic and continuum models. See [17,37] for a review of many of the existing methods. One class of such methods is based on a domain decompositions (DD) strategy, in which one explicitly divides the system into two types of subdomains, modeled separately by atomistic and continuum models. For instance, Mullins and Dokainish [41] proposed such a hybrid method in which a finite element linear elasticity model is used to provide boundary conditions for the atomistic region. Later, Kohlhoff et al. [27] proposed a more delicate coupling method, called the finite element method combined with atomistic modeling (FEAt), which couples linear elasticity model with molecular statics/dynamics. In FEAt, the mesh at the interface is gradually refined to the atomic scale so that the finite element nodes coincide with the atoms. An overlapping domain is created at the interface so that one model can provide the displacement boundary condition to the other. Another similar example is the blending method [5]. For dynamics problems, the DD approach has to be combined with an appropriate boundary condition

* Corresponding author.

E-mail addresses: xli@math.psu.edu (X. Li), zjysma@rit.edu (J.Z. Yang), weinan@math.princeton.edu (W. E).

¹ Research supported by NSF Grant DMS-0609610 and Alfred F. Sloan Fellowship.

² Research supported by in part by ONR Grant N00014-01-1-0674.

for the atomistic model, to take into account the atoms that have been replaced by the continuum description. This idea was first pursued in the work of E and Huang [15,16] for simplified models, in which efficient boundary conditions were obtained based on minimizing phonon reflection. Later, Wagner and Liu and their coworkers proposed the bridging scale method (BSM) [56,52], which uses a projection operator to connect molecular dynamics to the continuum elasto-dynamics model. At the interface, the boundary condition for molecular dynamics [55,25] was adopted to serve as the coupling condition. Using the same framework, To and Li [54] proposed another type of boundary condition analogous to the perfectly matched layers (PML) used in wave propagation problems.

Another class of methods are based on a variational approach. The observation is that both the atomistic and continuum models have a corresponding energetic formulation. For static problems, one successful approach is the quasi-continuum (QC) method [51,46,47,26,39]. The method consists of selecting a subset of atoms, called representative atoms, with which the displacement of the entire system can be approximated using linear interpolation, and an energy summation rule, which computes an approximation to the total energy of the system by visiting only a small number of atoms. The problem is then reduced to finding the mechanical equilibrium with respect to the approximate energy. The formalism was later extended to couple with continuum defect models in the coupled atomistic and discrete dislocation plasticity model (CADD) [48,49]. For dynamics problems, the first energy based method is the macro atomistic *ab initio* dynamics method (MAAD) [1,8], which simulates fracture dynamics using linear elasticity on the large scale together with molecular dynamics and quantum mechanical tight-binding model to resolve the crack tip behavior. The starting point of this method is to construct a total Hamiltonian that properly takes into account the total energy in all three regions. One then writes down the equations of motion using Hamilton's principle. In such an energetic formulation, the energy in the interior of each subdomain is often well defined. The energy at the interfaces, however, has to be calculated carefully. In MAAD, this is done by proper weighting. Another idea, proposed by Belytschko and Xiao, in their bridging domain method (BD) [6,58], is to create an overlapping region, in which the displacement is constrained using the finite element nodal values, and the energy is defined using a linear combination of the elastic strain energy and the atomic potential energy. A more first-principle based approach is the coarse-graining molecular dynamics method (CGMD) [44,43], in which the effective Hamiltonian for a pre-defined set of coarse-grain variables is obtained by integrating out the remaining degrees of freedom in the partition function. One main difficulty with this kind of variational approach is that it is unclear how to extend it to include thermal effects, particularly for systems when temperature is non-uniform.

The present work is a continuation of the long series of paper which began in [34]. The main objective of this series of paper is to develop a coupled atomistic/continuum formulation for studying the dynamics of solids at finite temperature, with good error control. The overall strategy is described in [34], and is based on a general framework for multiscale modeling – the heterogeneous multiscale method (HMM) [13,14]. What distinguishes our method from others is that the formulation is based on the conservation laws of mass, momentum and energy. The advantage of such a conservation law-based formulation is that it is completely general, and it is common to both the continuum and atomistic models. In particular, such conservation laws can be rigorously derived from molecular dynamics, as was shown in [34]. This gives a natural starting point for coupling.

As was pointed out above, the next difficulty is the coupling condition at the atomistic/continuum interface. An ideal coupled model should offer the same accuracy as the full atomistic model. An approximate coupling condition will introduce coupling error besides the numerical discretization error. These errors are manifested, for instance, in the force oscillation and ghost force observed in some methods for static problems, and phonon reflections for dynamics problems. How to minimize such coupling error has been the main subject of interest. For static problems, this has been carefully discussed and analyzed numerically for several existing methods in [40].

Looking into this problem, one quickly finds that the issue of boundary conditions for molecular dynamics simulation has not been adequately addressed in general. The most well-known problem is associated with the reflection of phonons at the boundary. But the issue is not just the elimination of phonon reflection, there is also the issue of taking thermal energy from the boundary in order to maintain a finite temperature. In principle, the exact boundary condition can be derived for linear problems, e.g. see [9,15,16,55,30]. Although these exact boundary conditions offer great insight, the formulas are quite non-local: They involve many atoms at the boundary, and their past history. In practice, they are quite expensive to use, particularly for real three-dimensional problems.

A consistent coupling of the atomistic and continuum models can be achieved by reformulating the molecular dynamics models as a set of conservation laws, expressed in the same form as the continuum models [34]. As a result, the coupling is at the level of flux functions, including mass flux, stress and energy flux. This coupling method will be integrated with a finite volume method, in which the numerical flux will be computed directly from the atomistic model. For the boundary condition, the main issue is to find the right compromise between accuracy and feasibility. This issue was initially explored in [15,16] and pursued further systematically in [35,36,30]. The idea is to find local approximations that are computationally more efficient. In addition, a variational formulation is used to find local boundary conditions with optimal accuracy. One main purpose of the present paper is to combine these boundary conditions with the general coupling framework proposed in [34]. The novel aspect in our approach is to define a mechanical equilibrium state, around which a linearization is done. On one hand, this greatly simplifies the linearization procedure. On the other hand, it will preserve a mechanical equilibrium state, which in the static case, has been demonstrated as an indication of uniform accuracy [18].

The second part of the paper focuses on the application to the propagation of brittle cracks. Although such problems have been studied extensively using molecular dynamics models, e.g. see [11,22,23,38], the results are mostly limited to the

behavior of the crack tip in the presence of an existing loading environment. These atomistic-based methods are unable to treat the dynamic loading from remote boundaries, or the interaction of the stress waves with the crack tip. Problems of this type involve both atomic level events and continuum scale processes, and they represent many of the challenges in multi-scale material modeling. This has been the main motivation for developing the current multiscale method.

In this paper, we will discuss the coupling method for the zero temperature case, where the continuum region is assumed to be at zero temperature, leaving the case of finite temperature to future publications. The paper is organized as follows: In Section 2, we describe both the continuum and atomistic models to be used in the multiscale approach. This is followed by a discussion of the coupling conditions in Section 3. Application to the crack problems is presented in Section 4.

2. Atomistic and continuum models

Our computation involves models at both macroscopic and microscopic scales: elasto-dynamics on the macroscopic scale, describing the evolution of the elastic field, and molecular dynamics at the atomic scale, providing the constitutive data based on detailed atomic interactions. In this section, we briefly present the equations underlying these models.

In molecular dynamics (MD) models, the system is described by the position and momentum of each individual atom in the system. For crystalline solids, the underlying lattice structure defines the reference position, R_i . The displacement is given by $\mathbf{u}_i = \mathbf{x}_i - R_i$; \mathbf{x}_i is the actual position of atom i . The dynamics of the atoms obey Newton's law:

$$\begin{cases} \dot{\mathbf{x}}_i = \mathbf{v}_i, \\ m_i \dot{\mathbf{v}}_i = -\nabla_{\mathbf{x}_i} V, \end{cases} \quad (1)$$

where m_i denotes the mass of the i th atom, which will be set to unity for simplicity, \mathbf{v}_i is the velocity, and $V(\mathbf{x}_1, \mathbf{x}_2, \dots, \mathbf{x}_N)$ is the interatomic potential. One example is the embedded atom model (EAM) [12] type of potential that takes the form:

$$V = \frac{1}{2} \sum_i \sum_j \phi_{t_i t_j}(r_{ij}) + \sum_i F_{t_i}(\bar{\rho}_i), \quad \bar{\rho}_i = \sum_{j \neq i} \rho_{t_j}(r_{ij}).$$

Here t_i indicates the atom type and $\mathbf{r}_{ij} = \mathbf{x}_i - \mathbf{x}_j$ with r_{ij} being the magnitude. The first term describes the pairwise interaction, and the second term, called the embedded energy, depends on the local electron density, $\bar{\rho}_i$.

In practice, most empirical potentials have the following properties. First, they can be written as,

$$V = \sum_i V_i(\mathbf{u}_1, \mathbf{u}_2, \dots, \mathbf{u}_N), \quad (2)$$

i.e. the energy at each atom. Secondly, the empirical potentials usually have a cut-off distance, r_{cut} : Atoms do not directly interact if their distance is bigger than the cut-off radius. This implies that,

$$\nabla_{\mathbf{x}_i} V_i = 0, \quad \text{if } r_{ij} > r_{\text{cut}}.$$

Finally, one can write the interatomic force on each atom as,

$$\mathbf{f}_i = -\nabla_{\mathbf{u}_i} V = \sum_{j \neq i} \mathbf{f}_{ij}, \quad (3)$$

and \mathbf{f}_{ij} obeys Newton's third law, $\mathbf{f}_{ji} = -\mathbf{f}_{ij}$.

For the continuum equations, they are usually formulated in the Lagrangian coordinate as well. Here we denote by \mathbf{x} the reference coordinates of the solid and $\mathbf{y} = \mathbf{x} + \mathbf{u}(\mathbf{x}, t)$, the position after deformation, with \mathbf{u} being the displacement. Then the dynamics of a solid system can be described by the equation of elasto-dynamics,

$$\begin{cases} \rho_0 \frac{\partial^2 \mathbf{u}}{\partial t^2} = \nabla \cdot \boldsymbol{\sigma}, \\ \rho_0 \frac{\partial e}{\partial t} = -\nabla \cdot \mathbf{J}, \end{cases} \quad (4)$$

where ρ_0 is the initial density, $\boldsymbol{\sigma}$ is the first Piola–Kirchhoff stress tensor, e is the energy, and \mathbf{J} is the energy flux. Although the current paper only focuses on problems at zero temperature, in which case the energy equation is not needed, it is still included here so that we can discuss the extension to more general cases.

In a multiscale setting, it is important that the continuum equation be consistent with the underlying atomistic model. For dynamics at zero temperature, the equations of elasto-dynamics have been derived for perfect crystals, for which the atomistic model can be viewed as difference equations. Therefore, continuum equations in the form of PDEs can be found by assuming that the solution is smooth. This is pursued by E and Ming [19], Arnd and Griebel [3], Tang et al. [53] and Chen and Fish [10].

For computational purposes, we rewrite the equation in the form of a set of conservation laws,

$$\begin{cases} \partial_t \mathbf{A} - \nabla_{\mathbf{x}} \mathbf{V} = 0, \\ \rho_0 \partial_t \mathbf{V} - \nabla_{\mathbf{x}} \cdot \boldsymbol{\sigma} = 0, \\ \rho_0 \partial_t e + \nabla \cdot \mathbf{J} = 0, \end{cases} \quad (5)$$

Here $\mathbf{A} = \mathbf{I} + \nabla \mathbf{u}$ is the deformation gradient, \mathbf{v} is the velocity. The first equation in (5) describes the time evolution of the deformation; the second is the conservation of momentum.

In the following section, we will describe how to combine these two models to develop a multiscale method.

3. Coupling condition of the atomistic and continuum models

Here we discuss how the two models can be integrated to describe multiscale material processes across physical scales. The heterogeneous multiscale method [13,14] distinguishes two types of coupling: Type B problems where there is scale separation between the fine and coarse scales, and type A problems, in which the coarse scale model is refined to fine scale model in areas where the fine scale events need to be resolved explicitly, creating an interface between the two models.

For the current problem, both of these ideas will be implemented. To begin with, the entire computational domain is decomposed into two subdomains: an *atomistic region*, denoted by Ω_j , in which molecular dynamics is used to resolve local defects, and a *continuum region*, denoted by Ω_c , away from the defects in which the system is modeled by the continuum model. This is illustrated in Fig. 1.

In each subdomain, the problem is treated as follows:

1. Within the continuum region, the problem is regarded as a type B problem, and the role of the MD is to provide the constitutive relation directly based on the atomistic model and the continuum equation in turn imposes constraints on the atomistic model.
2. Within the atomistic region, we keep track of the trajectories of the constituent atoms for the entire simulation period.
3. At the interface, an explicit coupling condition will be used to provide boundary conditions for both the continuum model and the atomistic system. Namely, it is treated as a type A problem.

This will be discussed in full details in the following sections.

3.1. Atomistic/continuum coupling in the continuum region: Atomistic-based constitutive modeling

In the continuum region, the MD model will be coarse-grained to the continuum model (5) with the average momentum and energy as the main variables. In this case, the coupling procedure has been discussed in [13,34,57], and we will briefly describe some main components here. First, based on the Irving–Kirkwood formula [24], one can show that the MD model can be reformulated into a set of conservation law, similar to the continuum model (4). More specifically, let ρ_0 be the density at reference state, and we define the local momentum and energy,

$$\begin{cases} \rho_0 \tilde{\mathbf{v}}(\mathbf{x}, t) = \sum_i m_i \dot{\mathbf{x}}_i(t) \delta(\mathbf{x} - \mathbf{R}_i), \\ \tilde{e}(\mathbf{x}, t) = \sum_i [m_i \frac{1}{2} \mathbf{v}_i^2 + V_i] \delta(\mathbf{x} - \mathbf{R}_i). \end{cases} \quad (6)$$

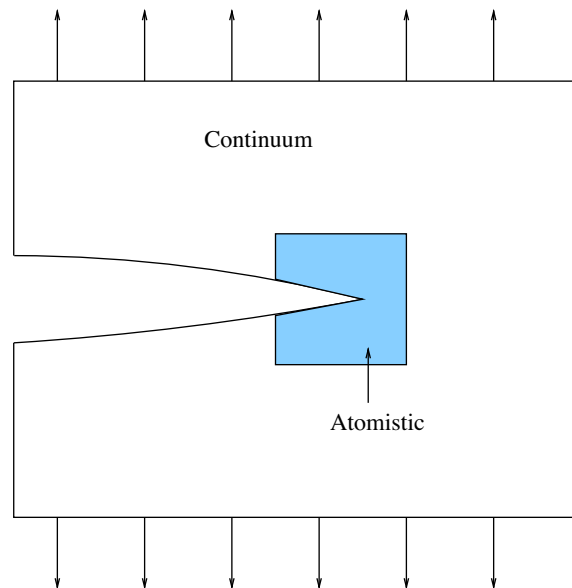


Fig. 1. An example of the decomposition of the domain for a system with an opening crack: a subdomain is selected near the crack tip which will be modeled atomistically. The surrounding region is modeled by continuum elasto-dynamics.

As a result, the total momentum and energy in a control volume can be easily computed by an integral. Furthermore, one can derive conservation laws for the local momentum and energy,

$$\begin{cases} \rho_0 \partial_t \tilde{\mathbf{v}} - \nabla \cdot \tilde{\boldsymbol{\sigma}} = 0, \\ \rho_0 \partial_t \tilde{e} + \nabla \cdot \tilde{\mathbf{j}} = 0. \end{cases} \tag{7}$$

where,

$$\begin{cases} \tilde{\boldsymbol{\sigma}}(\mathbf{x}, t) = \frac{1}{2} \sum_{i \neq j} \mathbf{f}_{ij} \otimes (\mathbf{R}_i - \mathbf{R}_j) \times \int_0^1 \delta(\mathbf{x} - (\mathbf{R}_j + \lambda(\mathbf{R}_i - \mathbf{R}_j))) d\lambda, \\ \tilde{\mathbf{j}}(\mathbf{x}, t) = \frac{1}{4} \sum_{i \neq j} (\mathbf{v}_i + \mathbf{v}_j) \cdot \mathbf{f}_{ij} \otimes (\mathbf{R}_i - \mathbf{R}_j) \times \int_0^1 \delta(\mathbf{x} - (\mathbf{R}_j + \lambda(\mathbf{R}_i - \mathbf{R}_j))) d\lambda. \end{cases} \tag{8}$$

We are now in a position to describe the multiscale coupling method. The coupling strategy is quite straightforward: we first pick a macro solver for the macroscale Eq. (5). Here a shock-capturing scheme is used, which has been a central topics for solutions of hyperbolic conservation laws [20,29]. Examples include the central schemes and discontinuous Galerkin methods. They have been implemented in our previous work [34,57]. They have the advantage of correctly predicting shock waves, and minimizing spurious oscillations. For dynamics of solid, this is extremely important in studying the impact of shock waves on local defects. Most of these shock-capturing schemes can be written in a conservative form, with numerical solutions defined at the cell centers as cell averages and numerical fluxes defined at the cell interfaces. In this paper, we will choose the Roe scheme to compute the numerical fluxes. The idea is to linearize the equations at each cell edge using the left and right states. In computing the numerical flux, one starts with the flux function from one side of the interface, and then corrections are made based on the wave characteristics of the linearized equation. The details of the linearization for the elasto-dynamics model (5) are given in the Appendix A.

In the multiscale setting, the stress and energy flux in each cell, which will appear in the numerical fluxes, are obtained directly from the atomistic model, either from a direct MD simulation, or from an asymptotic approximation. On the other hand, the macroscale variables, including the deformation gradient, momentum and energy, will be used to constrain the atomistic system. This procedure can be demonstrated from Fig. 2. Within each cell, we first initialize an atomistic system with atoms positioned at the lattice sites. This paper only focuses on zero temperature case, in which case there is no finite size effect. So only the atoms in one unit atomic cell is needed. Second, using the deformation gradient, \mathbf{A} , one deforms the atomic cell uniformly. One can then compute the stress using a periodic boundary condition with respect to the deformed box. This is the standard Cauchy–Born approximation. It estimates the local stress at that point. For problems at finite temperature, one can apply a thermostat to bring the system to the desired temperature, and then sample the stress by time averaging (see discussion in [34]). An alternative is to use the harmonic approximation, in which the Cauchy–Born rule becomes the leading term [28]. Comparing to the conventional numerical procedure, we have used atomistic model as a supplemental component in each cell to supply the constitutive data. In the continuum region, the mesh size can be much larger than the atomic spacing, offering a great deal of computational savings. The overall method is demonstrated in Fig. 2.

3.2. Atomistic/continuum interface condition: From atomistic to continuum

We now turn to the interface between the atomistic and continuum regions. To achieve a consistent overall coupling condition, we start with the full atomistic model for the entire sample. We will adopt a finite volume formulation, similar to the derivation of traditional continuum mechanics models and the finite volume method in the previous section. We divide the entire computational domains, Ω , into a number of cells: $\Omega = \cup_{\alpha} C_{\alpha}$. For any cell C_{α} , we define the average momentum and energy,

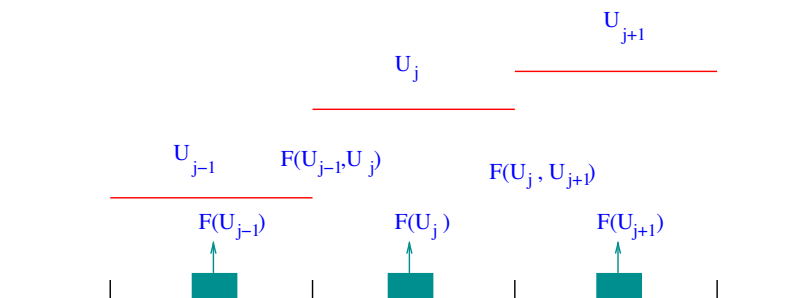


Fig. 2. An illustration of the coupling method in the continuum region. A finite volume discretization is used. For each cell, we compute the flux $F(U_j)$ (e.g. the stress) based on the atomistic model, which will then be used in the calculation of the numerical fluxes, $F(U_j, U_{j+1})$.

$$\begin{aligned} \mathbf{p}_\alpha &= \frac{1}{|C_\alpha|} \sum_{i \in C_\alpha} m_i \mathbf{v}_i, \\ E_\alpha &= \frac{1}{|C_\alpha|} \sum_{i \in C_\alpha} \left[V_i + \frac{1}{2} m_i \mathbf{v}_i^2 \right]. \end{aligned} \tag{9}$$

Substituting (1) into the equation above, we find that,

$$\begin{aligned} \frac{d}{dt} \mathbf{p}_\alpha &= \frac{1}{|C_\alpha|} \sum_{\substack{i \in C_\alpha \\ j \notin C_\alpha}} \mathbf{f}_{ij}, \\ \frac{d}{dt} E_\alpha &= \frac{1}{|C_\alpha|} \sum_{\substack{i \in C_\alpha \\ j \notin C_\alpha}} \frac{1}{2} \mathbf{f}_{ij} \cdot (\mathbf{v}_i + \mathbf{v}_j). \end{aligned} \tag{10}$$

This is reminiscent of the finite volume formulation of continuum mechanics models, and the terms on the right hand side can be viewed as the discrete analog of the momentum and energy fluxes.

Near the local defects, we retain the full atomistic description and Eq. (10) does not yield additional information. Near the interface, we compute the fluxes based on the following strategy. For the cell edges at the interface, the fluxes are computed directly based on the atom position and velocity using (10), averaged over the time interval $(t, t + \Delta t)$; Δt is the step size for the continuum model. This procedure is shown in Fig. 3. For the cell edges inside the continuum region, the fluxes are computed from the shock-capturing method, in which the stress are obtained directly from MD. Since the problem is assumed to be at zero temperature, the Cauchy–Born approximation can be used.

To better illustrate the coupling method, let us consider a two-dimensional domain, which is divided into rectangular cells. Let $\mathbf{v}_{J+\frac{1}{2},K+\frac{1}{2}}$ be the volume average of the velocity,

$$\rho_0 \mathbf{v}_{J+\frac{1}{2},K+\frac{1}{2}} = \frac{1}{|C_{JK}|} \sum_{i \in C_{JK}} m_i \mathbf{v}_i, \tag{11}$$

in the (J,K) th cell, denoted by C_{JK} . $|C_{JK}| = \Delta x \Delta y$.

Using (1), one finds that,

$$\frac{d}{dt} \rho_0 \mathbf{v}_{J+\frac{1}{2},K+\frac{1}{2}} = \frac{1}{|C_{JK}|} \sum_{\substack{i \in A_{JK} \\ j \notin A_{JK}}} \mathbf{f}_{ij}. \tag{12}$$

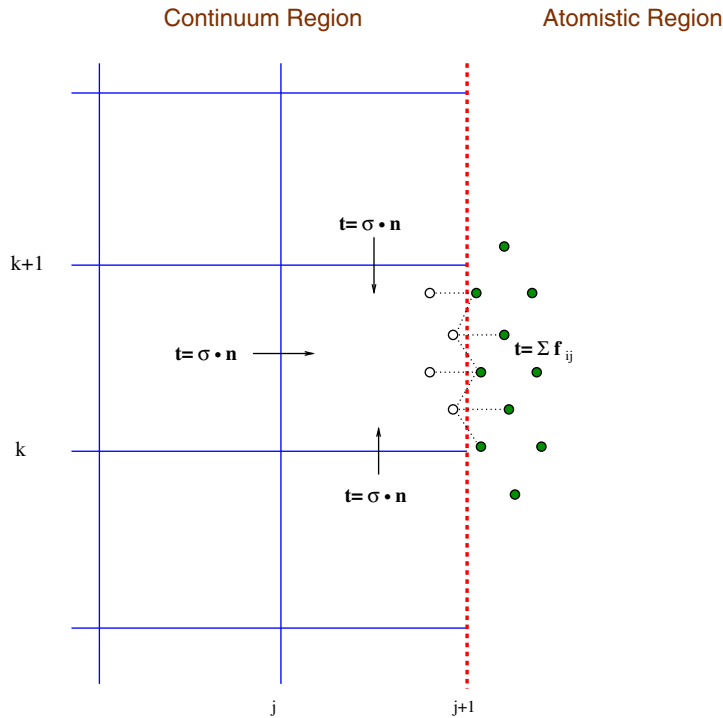


Fig. 3. A schematic of the atomistic/continuum coupling strategy: a finite volume method is applied to a cell next to the interface. For the edges that are inside the continuum region, the fluxes, e.g. the traction \mathbf{t} , are computed from the continuum model by an approximate Riemann solver; At the edge between the atomistic and continuum regions, the flux is computed directly from molecular dynamics.

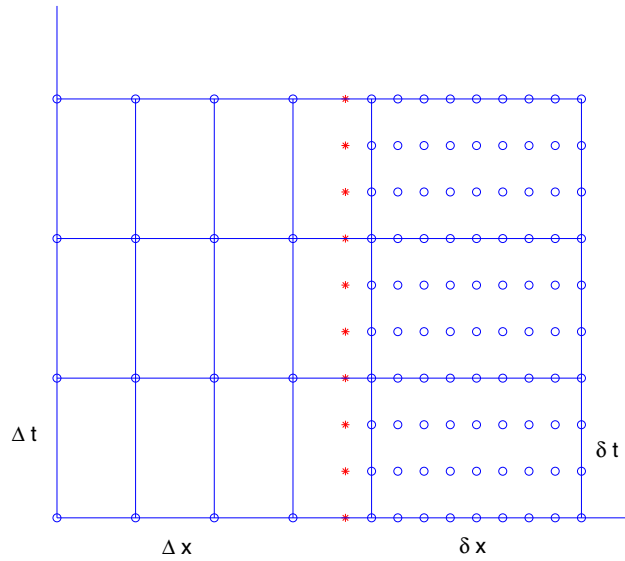


Fig. 4. An illustration of the multiscale method. The circles represent the atoms in the atomistic region. The stars are the atoms at the interface that need to be reconstructed to provide the boundary condition for the atomistic model.

Similarly, we have,

$$\frac{d}{dt} E_{J+\frac{1}{2},K+\frac{1}{2}} = \frac{1}{2|C_{JK}|} \sum_{\substack{i \in A_{JK} \\ j \notin A_{JK}}} \mathbf{f}_{ij} \cdot (\mathbf{v}_i + \mathbf{v}_j). \tag{13}$$

From these calculations, we find the momentum flux (traction) and energy flux across the cell interface. Integrating (12) in time, one gets,

$$\rho_0 \mathbf{v}_{J+\frac{1}{2},K+\frac{1}{2}}(t + \Delta t) = \rho_0 \mathbf{v}_{J+\frac{1}{2},K+\frac{1}{2}}(t) + \frac{\Delta t}{\Delta x} (\mathcal{F}_{J+1,K+\frac{1}{2}} - \mathcal{F}_{J,K+\frac{1}{2}}) + \frac{\Delta t}{\Delta y} (\mathcal{F}_{J+\frac{1}{2},K+1} - \mathcal{F}_{J+\frac{1}{2},K}). \tag{14}$$

Here \mathcal{F} corresponds to the net fluxes across each cell interface within the time interval $(t, t + \Delta t)$.

This coupling method has the following advantage: (1) it is formulated directly based on conservation laws, which are consistent with the continuum model and (2) we avoid the usage of stress at the interface, whose definition has been rather controversial.

The remaining question is how to impose the boundary condition to the atomistic region. The interface condition should reconstruct the displacement and velocity of the atoms at the interface so that the forces on the atoms in the atomistic region can be computed. This will be discussed in the next section.

3.3. Atomistic/continuum interface condition: From continuum to atomistic

The next step in the coupling procedure is to impose boundary condition for the atomistic region. Ideally the boundary condition should take into account the atoms that are already in the atomistic region, and the atoms that have been removed in the continuum region.

For this purpose, we will divide the atoms into two groups: the set Ω_i , including those atoms in the atomistic region, and the set Ω_j , which contains the surrounding atoms lying in the continuum region. For clarity, we will denote the displacement of those two groups of atoms as \mathbf{u}_i and \mathbf{u}_j , respectively. Similarly, we define M_i and M_j as the mass matrices.

Since the displacement \mathbf{u}_j in the continuum region is not explicitly involved in the computation, they have to be reconstructed from their average displacement and velocity by interpolation. In practice, since most atomic potentials have a short cut-off distance, only the atoms close to the interface need to be reconstructed. The reconstructed values at the current time step t_n are denoted by $\bar{\mathbf{u}}_j$ and $\bar{\mathbf{v}}_j$, respectively. Similarly we define $\bar{\mathbf{u}}_i$ and $\bar{\mathbf{v}}_i$ as the interpolation from the cell averages, and $\bar{\mathbf{u}}_i$ and $\bar{\mathbf{v}}_i$ as the remaining parts. Here $\bar{\mathbf{u}}$ is regarded as the coarse scale component, which depends on the mesh size, the $\bar{\mathbf{u}}$ is the fine scale component.

An schematic illustration of the coupling of the continuum and atomistic models is given in Fig. 4. The mesh size for the continuum region equals to a few atomic spacings, $\Delta x = K\delta x$. As a result, each cell overlaps with several atom units. In addition, the step size for the continuum region is equal to a number of MD time steps, $\Delta t = M\delta t$. Therefore, during a macro time step $t \in (t_n, t_{n+1})$, the coupling of the two models is follows: In order to apply the finite volume method in the continuum

region, one needs to compute the fluxes at the interface, which depend on the coordinate and momentum of the atoms there. On the other hand, to evolve the atoms in the atomistic region, the position of those atoms in the continuum region that are close to the interface have to be reconstructed.

In principle, the interface condition can be obtained from solving the following initial value problem: For $t \in (t_n, t_{n+1})$,

$$\begin{cases} M_J \ddot{\mathbf{u}}_J = -\nabla_{\mathbf{u}_J} V \\ M_I \ddot{\mathbf{u}}_I = -\nabla_{\mathbf{u}_I} V \end{cases} \quad (15)$$

with initial conditions,

$$\mathbf{u}_J(t_n) = \bar{\mathbf{u}}_J, \quad \mathbf{v}_J(t_n) = \bar{\mathbf{v}}_J.$$

The initial condition for \mathbf{u}_I and \mathbf{v}_I are obtained from the previous MD step. Since we are only computing the displacement and velocity at the interface for a short time period Δt , the boundary conditions for \mathbf{u}_J at the remote boundaries are neglected.

This is another similarity to the continuum model: It is similar to the Godunov scheme for the continuum PDEs [21], where at each time step, one first reconstructs the solution, and then solves an initial values problem to find the flux functions at each cell interface (a Riemann problem). In particular, here in the continuum region, we will neglect waves of smaller wavelength at each macro time step, as is done in finite volume methods for conservation laws.

Similar to a Riemann problem, it is usually difficult to find the exact solution, and a proper linearization is often needed to obtain an approximate solution. For instance for the Roe scheme [42], one starts with the flux function from one neighboring cell, and makes corrections based on the wave characteristics, to properly take into account waves in the upwind/downwind direction. For the MD model, we will retain the nonlinear atomic interaction in the atomistic region, which is needed to describe local defects, and linearize the interaction involving atoms in the continuum region. In this case, the traditional harmonic approximation around the reference state for the entire system (e.g. see [4,7]) is not applicable. For example, the atoms around an open crack are usually displacement far from the reference positions, and the conventional harmonic approximation would lead to large error at the interface. Our main idea is to introduce a harmonic approximation near a mechanical equilibrium. We first define the following mapping

$$\mathbf{u}_J^* = \mathcal{S}(\mathbf{u}_I)$$

where \mathbf{u}_J^* satisfies

$$\nabla_{\mathbf{u}_J} V(\mathbf{u}_J, \mathbf{u}_J^*) = 0. \quad (16)$$

Namely, the continuum region is at a mechanical equilibrium. In principle, one can also choose other mechanical equilibrium states using different boundary conditions at the remote boundaries.

In practice, it is difficult to compute $\mathcal{S}(\mathbf{u}_I)$ directly. A linear approximation will be used, which is given by

$$\mathcal{S}(\mathbf{u}_I) \approx B_{JI} \mathbf{u}_I, \quad B_{JI} = -D_{JJ}^{-1} D_{JI}. \quad (17)$$

Here the matrix D_{JJ} contains the force constant associated with the atoms in Ω_J , and D_{JI} contains the force constant associated with the atoms lying one different sides of the interface. The matrix B_{JI} , usually sparse, can be computed efficiently using lattice Green's functions [32]. It can be viewed as an extrapolation. In particular, when the atoms in Ω_I is uniformly deformed, it should produce the exact solution.

Next we approximate the potential energy around this equilibrium state,

$$V(\mathbf{u}_I, \mathbf{u}_J) \approx V(\mathbf{u}_I, B_{JI} \mathbf{u}_I) + \frac{1}{2} (\mathbf{u}_J - B_{JI} \mathbf{u}_I)^T D_{JJ} (\mathbf{u}_J - B_{JI} \mathbf{u}_I). \quad (18)$$

Similar to the standard harmonic approximation, this approximation is valid when the displacement field in the continuum region is smooth.

This approximate energy will be used to replace the potential energy in the Hamiltonian. Using the Hamilton's principle, we obtain the following equations,

$$M_J \ddot{\mathbf{u}}_J = -D_{JJ} (\mathbf{u}_J - B_{JI} \mathbf{u}_I) \quad (19)$$

and,

$$M_I \ddot{\mathbf{u}}_I = -\nabla_{\mathbf{u}_I} V(\mathbf{u}_I, B_{JI} \mathbf{u}_I) + B_{IJ} D_{JJ} (\mathbf{u}_J - B_{JI} \mathbf{u}_I). \quad (20)$$

Eqs. (19) and (20) constitute the basis for deriving the interface condition. We first separate out the 'continuum part' of the solution. Let $\bar{\mathbf{u}}_I(t) = \bar{\mathbf{u}}_I(t_n) + (t - t_n) \bar{\mathbf{v}}_I(t_n)$, and

$$\mathbf{w}_J(t) = B_{JI} \bar{\mathbf{u}}_I(t). \quad (21)$$

This will be regarded as part of the solution, which can be computed on-the-fly from the atomistic region. Let the remaining part be \mathbf{q}_J ,

$$\mathbf{q}_J = \mathbf{u}_J - \mathbf{w}_J. \tag{22}$$

In addition, we let

Subtracting Eq. (21) from (19), we find,

$$\begin{cases} M_J \ddot{\mathbf{q}}_J = -D_{JJ}(\mathbf{u}_I - \bar{\mathbf{u}}_I) - D_{JJ} \mathbf{q}_J \\ \mathbf{q}_J(t_n) = \bar{\mathbf{u}}_J - B_{JI} \bar{\mathbf{u}}_I, \\ \dot{\mathbf{q}}_J(t_n) = \bar{\mathbf{v}}_J - B_{JI} \bar{\mathbf{v}}_I. \end{cases} \tag{23}$$

We will further decompose it into two separate problems

$$\begin{cases} M_J \ddot{\mathbf{q}}_J^{(1)} = -D_{JJ} \mathbf{q}_J^{(1)} \\ \mathbf{q}_J^{(1)}(t_n) = \bar{\mathbf{u}}_J - B_{JI} \bar{\mathbf{u}}_I, \\ \dot{\mathbf{q}}_J^{(1)}(t_n) = \bar{\mathbf{v}}_J - B_{JI} \bar{\mathbf{v}}_I, \end{cases} \tag{24}$$

and

$$\begin{cases} M_J \ddot{\mathbf{q}}_J^{(2)} = -D_{JJ} \mathbf{q}_J^{(2)} - D_{JI} \bar{\mathbf{u}}_I, \\ \mathbf{q}_J^{(2)}(t_n) = \mathbf{0}, \dot{\mathbf{q}}_J^{(2)}(t_n) = \mathbf{0}. \end{cases} \tag{25}$$

The total displacement is then $\mathbf{q}_J = \mathbf{q}_J^{(1)} + \mathbf{q}_J^{(2)}$.

It follows directly from (24) that,

$$\mathbf{q}_J^{(1)} = K_{JJ}^{-1/2} \sin\left(K_{JJ}^{1/2}(t - t_n)\right) (\bar{\mathbf{v}}_J - B_{JI} \bar{\mathbf{v}}_I) + \cos\left(K_{JJ}^{1/2}(t - t_n)\right) (\bar{\mathbf{u}}_J - B_{JI} \bar{\mathbf{u}}_I). \tag{26}$$

Here $K_{JJ} = M_J^{-1} D_{JJ}$. The motivation of such a decomposition is two fold. First, if initially the continuum region is at equilibrium, then $\mathbf{q}_J^{(1)} = \mathbf{0}$. Namely this accounts for the mechanical imbalance between the two regions. Secondly since the initial condition is given by $\bar{\mathbf{u}}$ and $\bar{\mathbf{v}}$, the coarse scale part of the solution, we expect that $\mathbf{q}_J^{(1)}$ can be approximated by a Taylor expansion,

$$\mathbf{q}_J^{(1)} \approx [\bar{\mathbf{u}}_J - B_{JI} \bar{\mathbf{u}}_I] + (t - t_n) [\bar{\mathbf{v}}_J - B_{JI} \bar{\mathbf{v}}_I] - \frac{1}{2} (t - t_n)^2 K_{JJ} [\bar{\mathbf{u}}_J - B_{JI} \bar{\mathbf{u}}_I]. \tag{27}$$

Notice that all these terms on the right hand side can be computed locally near the interface, whereas in (26), all atoms in the continuum regions are involved.

Meanwhile, for (25), the solution can be written as,

$$\mathbf{q}_J^{(2)} = \int_0^{t-t_n} \alpha(\tau) \tilde{\mathbf{u}}_I(t - \tau) d\tau, \tag{28}$$

where the Laplace transform of the function α is given be,

$$\hat{\alpha}(\lambda) = -(\lambda^2 I + K_{JJ})^{-1} K_{JI}, \tag{29}$$

in which $K_{JI} = M_J^{-1} D_{JI}$. This is usually how an absorbing boundary condition is formulated [2,25,35,55]. Namely, one assumes that the surrounding region is initially at rest or at a mechanical equilibrium. One then finds the interface condition which implicitly takes into account the effect of the surrounding atoms.

Now we return to (20), which can be written as,

$$M_I \ddot{\mathbf{u}}_I = -\nabla_{\mathbf{u}_I} V(\mathbf{u}_I, B_{JI} \mathbf{u}_I) - D_{IJ} \mathbf{q}_J - D_{IJ} D_{JJ}^{-1} D_{JI} \tilde{\mathbf{u}}_I(t), \tag{30}$$

Substituting $\mathbf{q}_J^{(2)}$ into the equation above, we have,

$$-D_{IJ} \mathbf{q}_J^{(2)} = \int_0^{t-t_n} \beta(\tau) \tilde{\mathbf{u}}_I(t - \tau) d\tau,$$

where,

$$\beta = -D_{IJ} \alpha.$$

The memory kernel can be further simplified using an integration by parts,

$$-D_{IJ} \mathbf{q}_J^{(2)} = - \int_0^{t-t_n} \theta(\tau) \tilde{\mathbf{v}}_I(t - \tau) d\tau + \theta(0) \tilde{\mathbf{u}}_I - \theta(t - t_n) \tilde{\mathbf{u}}_I(t_n),$$

where,

$$\theta(t) = \int_t^{+\infty} \beta(\tau) d\tau. \tag{31}$$

One can verify that,

$$\theta(0) = D_{ij} D_{jj}^{-1} D_{ji}.$$

Therefore, we have the following coupling condition, in the form of a generalized Langevin equation (GLE),

$$M_i \ddot{\mathbf{u}}_i = -\nabla_{\mathbf{u}_i} V(\mathbf{u}_i, B_{ji} \mathbf{u}_i) - \int_0^{t-t_n} \theta(\tau) \tilde{\mathbf{v}}_i(t-\tau) d\tau - \theta(t-t_n) \tilde{\mathbf{u}}_i(t_n) + \mathbf{f}^{\text{ex}}, \tag{32}$$

where,

$$\mathbf{f}^{\text{ex}} = -D_{ij} \mathbf{q}_j^{(1)},$$

models the effect of the existing elastic field in the continuum region. It can be combined with the first term on the right hand side of (32). Namely,

$$-\nabla_{\mathbf{u}_i} V(\mathbf{u}_i, B_{ji} \mathbf{u}_i) - D_{ij} \mathbf{q}_j^{(1)} \approx -\nabla_{\mathbf{u}_i} V(\mathbf{u}_i, \mathbf{q}_j^{(1)} + B_{ji} \mathbf{u}_i).$$

In order to solve the GLE at the interface, the matrix B_{ij} and the function $\theta(t)$ have to be computed a priori. An important practical problem is that they are nonlocal in that all the atoms at the boundary are correlated. For the kernel function $\theta(t)$, the correlation is also nonlocal in time. Since the memory term has to be evaluated at each time step, this often leads to considerable computational overhead. Therefore, it is desirable to find local boundary conditions with reasonable accuracy. Since each entry of these matrices are associated with two atoms at the boundary, we can look for a local boundary condition by forcing,

$$B_{ij} = 0, \theta_{ij}(t) = 0,$$

if $|R_i - R_j| \geq r_c$, or $t \geq t_c$. Here r_c and t_c are pre-selected parameters. To find such a local approximation that has the best accuracy, we follow our previous approach of the variational boundary condition method (VBC) [31,33,30,35]. One way to define an objective function is to use the Green's function. The observation is quite simple: If the atoms at the boundary of the atomistic region are displaced according to a Green's function, then the displacement of the atoms outside the atomistic region should be given by the same Green's function, provided that the boundary condition is exact. Therefore a residual function can be defined when the approximation boundary condition is substituted. Finally, the optimal local approximation will be obtained by minimizing the residual. For more details, see [31].

Remarks:

1. This approach is built on a statics problem. When the system is initially uniformly deformed with a constant velocity, such state will be preserved by the interface condition. This is an important consistent property.
2. One key point here is that we perform the linearization around a mechanical equilibrium. As a result, there is no force term in the harmonic approximation. Comparing to the work Wagner and Liu [56], the interface condition is much easier to implement.
3. At finite temperature, a similar GLE can be derived with an additional forcing term, representing the phonons from the surrounding atoms [30].
4. It can be shown that the memory and the external force terms vanish when the distance to the interface is greater than the cut-off distance, and the GLE is reduced to the equation of MD. Therefore, the GLE can be viewed as an intermediate model bridging the atomistic and continuum descriptions.

We summarize the computational procedure as follows. For each macro time step (t_n, t_{n+1}) :

1. Compute the numerical fluxes at the cell edges inside the continuum region using the Roe scheme (38).
2. Use an interpolation procedure to compute $\tilde{\mathbf{u}}_j, \tilde{\mathbf{v}}_j$ and $\tilde{\mathbf{v}}_i$.
3. For the MD time steps
 - Solve the Eq. (32) using the results from the previous step as the initial condition.
 - Save $\tilde{\mathbf{v}}_i$ at the same time to compute the memory term at the following steps.
 - Compute the fluxes at the atomistic/continuum interface using (10).
 - At the last step, average the fluxes to obtain the mean fluxes.
4. Use the conservative scheme (37) to update displacement and velocity in the continuum region.
5. Now the system has been evolved to $t = t_{n+1}$. Go to (1) unless the final time has been reached.

4. Numerical experiments

4.1. Shock propagation in a one-dimensional chain

As an example, we first consider a one-dimensional model of a linear chain connect by nonlinear springs,

$$m\ddot{u}_j = \varphi'(u_{j+1} - u_j) - \varphi'(u_j - u_{j-1}). \quad (33)$$

The function φ gives the energy stored in each spring. For the interface condition, we may assume that the atomistic region contains those atoms for which $j \geq 0$, and the rest of the atoms on the left are in the continuum region. In this case, $B_{jl} = 1$. The GLE is given by,

$$\begin{cases} m\ddot{u}_0 = \varphi'(u_1 - u_0) - \int_0^{t-t_n} \theta(t-s) \dot{v}_0(s) ds - \theta(t-t_n) \tilde{u}_0(t_n) + f^{\text{ex}}, \\ m\ddot{u}_j = \varphi'(u_{j+1} - u_j) - \varphi'(u_j - u_{j-1}), \quad j > 0. \end{cases} \quad (34)$$

The simulation starts with an existing shock, which will propagate through the interface. In the first experiment, the shock is inside the atomistic region and later moves into the continuum region, see Fig. 5. In the second experiment, the shock is initially in the continuum region, and later enters the atomistic region, see Fig. 6. One can see that despite the large gradient of the stress wave, the interface condition allows the shock waves to move through.

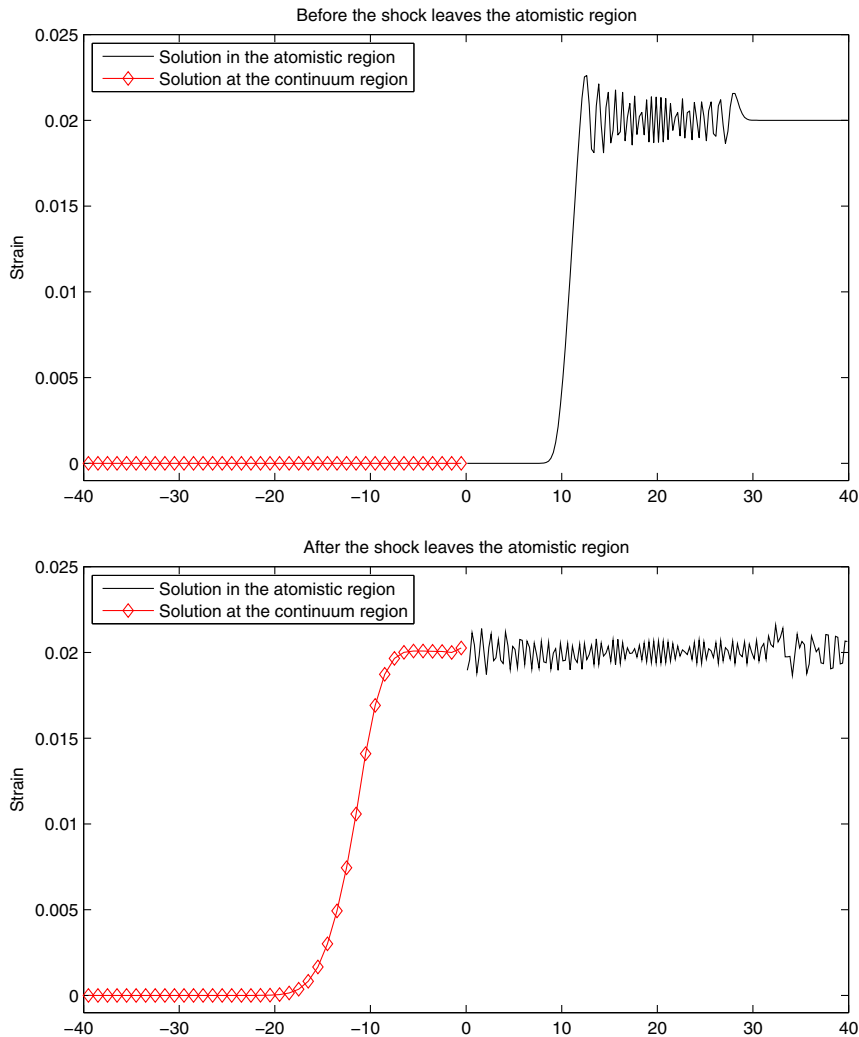


Fig. 5. A shock propagating from the atomistic region to the continuum region.

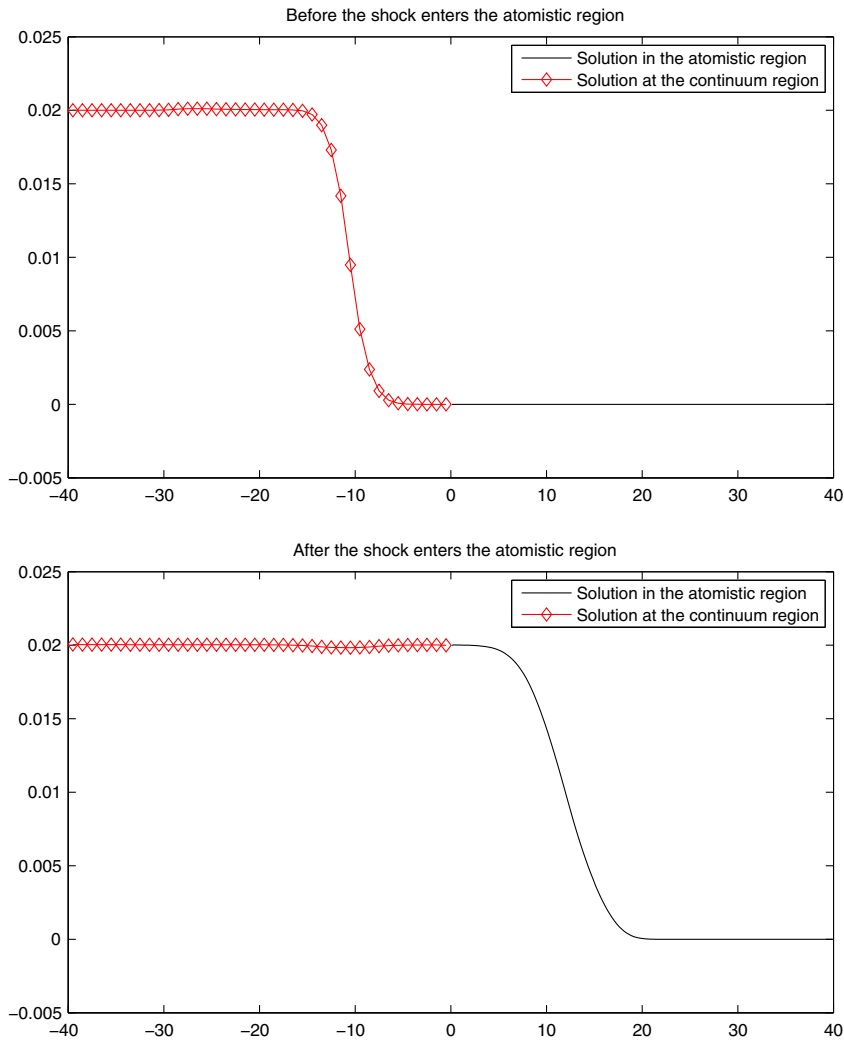


Fig. 6. A shock moving into the atomistic region from the continuum region.

4.2. Crack propagation in Iron-alpha

We now consider an opening crack in b.c.c. α -Fe. The atomic potential used here is the EAM potential developed by Shastry and Farkas [45]. The system studied consists of a 3D rectangular sample, with the three orthogonal axes being along [110], $[1\bar{1}0]$ and [001] directions, respectively. Along the third direction the system is assumed to be homogeneous, enforced by a periodic boundary condition. Therefore, the full continuum model can be reduced to a two-dimensional problem.

We start with an opening crack with elliptical shape, with displacement computed from the anisotropic linear elasticity solution [50], in which the elastic constants are computed directly from the EAM potential [45]. Initially the crack tip is placed at the center of the sample. The stress intensity factor is chosen based on the Griffith criterion, and the surface energy for [110] plane of α -Fe calculated from the EAM potential is $\gamma = 0.104 \text{ eV } \text{\AA}^{-2}$, which is close to the experimentally observed value [11].

The entire domain is discretized into a 200×200 mesh, of which, the 16×16 cells at the center overlap with the atomistic region. For the mesh size, we choose $\Delta x = 4\delta x$, and $\delta x = \sqrt{2}a_0$ with a_0 being the lattice constant. We also choose $\Delta t = 4\delta t$.

We examine two types of problems to check the coupling of two models. The first problem is the relaxation of the crack. And in the second problem, we examine the crack behavior under dilative loading applied at the boundary of the continuum region.

4.2.1. Relaxation of the crack tip region

First we investigate the relaxation process of a crack. A macroscopic traction boundary condition was applied such that the magnitude of the traction equals that of the solution of the linear elasticity problem, with the stress intensity factor $k_I = 1.0k_I^c$, where k_I^c is the critical stress intensity factor calculated from the Griffith criteria.

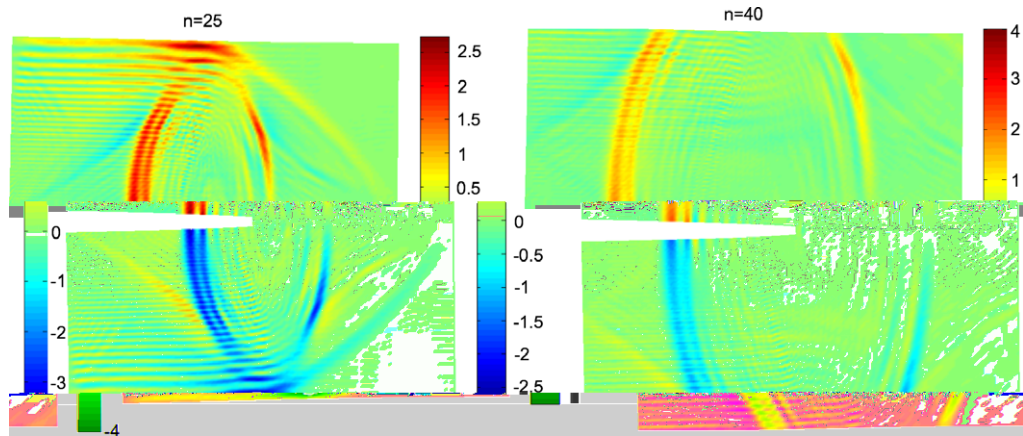


Fig. 7. Relaxation of the crack tip viewed in the MD region. The left figures: $t = 5$ ps; right figures: $t = 8$ ps. Two types of waves were emitted from the tip with square and elliptic profile, respectively. Majority of the two wave were transmitted to the continuum region through the interface coupling condition. Only small fraction of the waves were reflected back to the atomistic region due to the finite size of variational boundary condition used.

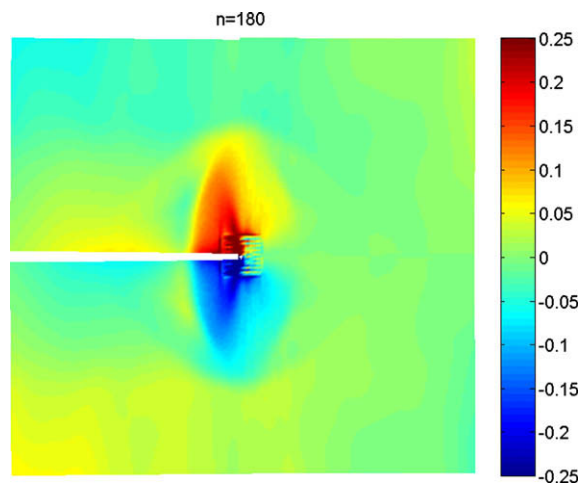


Fig. 8. Crack relaxation viewed in the overall computational domain, colored according to the second component of the velocity field. Values within the atomistic region were calculated from averaging. Snapshot was taken when $t = 45$ ps. The two types of wave fronts emitted from the MD region were preserved and kept propagating towards the outmost boundary.

In the MD region, as the crack started to relax, there are both high frequency and low frequency waves emitted from the crack tip. Most of the high frequency waves were absorbed by the MD boundary condition. These are waves that cannot be resolved by continuum resolution. However, small reflections can still be seen at the MD boundary. This can be attributed to the fact that in deriving the coupling condition (15), the fine scale displacement in the continuum region has been ignored, and that the size of the velocity history in the GLE (32) is limited by the size of the macro time step. For the low frequency waves, two types of the wave fronts can be seen: one is of diamond shape, typical in materials of cubic structure, and the other is elliptical, see Fig. 7.

As the system continues to relax, one can observe elastic waves emitted from the crack tip and propagate through the atomistic/continuum interface toward the continuum region. The two types of wave fronts were also observed in the continuum region, see Fig. 8.

Upon close inspection, the crack did not open in this example.

4.2.2. Crack under dilative loading

We also studied the case when dilative traction boundary condition for the continuum region is applied. Same as the previous example, the crack was initialized according to equilibrium elasticity solution with critical stress intensity factor $k_I = 1.0k_I^c$ for the whole simulation sample.

Meanwhile a dilative traction boundary condition corresponding to a specific stress intensity factor, $k_I = 2.0k_I^c$, was applied at the boundary of the continuum region. Shock waves are generated from the top and bottom boundary, and

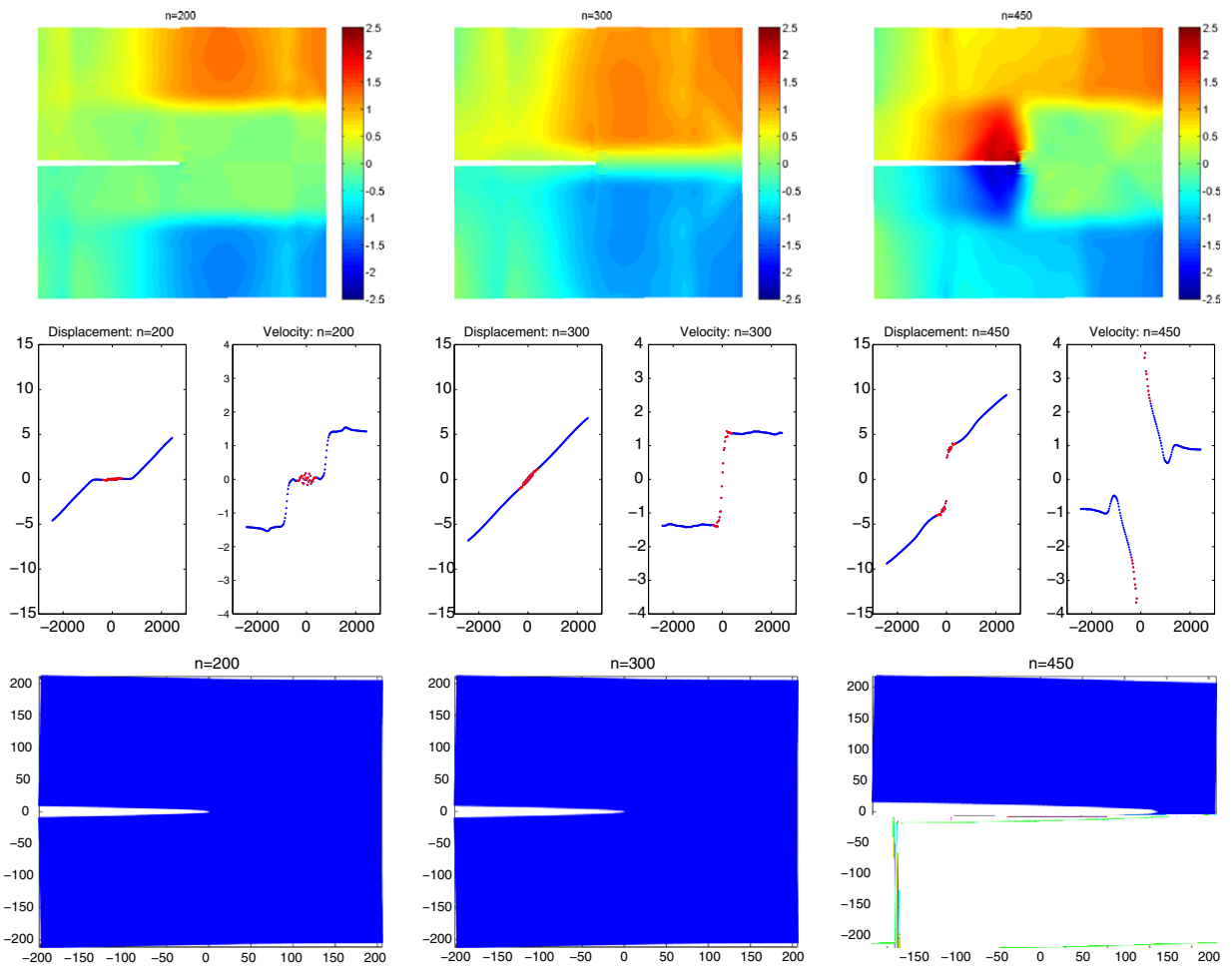


Fig. 9. First row: snapshots of velocity waves propagation from the top and bottom boundaries to the interior when dilative loading were applied. Snapshot were colored according to the second components of the velocity field. Waves came across and canceled out each other ahead of the crack tip and bounded back on the crack faces behind the crack tip. Values within the atomistic region were calculated by averaging; Second row: plots for the second components of displacements and velocities along a vertical line 3 macroscopic cell ahead of the crack tip. Red star dots represent values calculated in the atomistic region by averaging. Shock waves in velocity propagated from the two ends toward the center. The displacements increased linearly before the crack opened and separated from the center afterwards; Third row: snapshots of the crack tips viewed in the atomistic region. Crack stayed still before the shock waves arrived and the crack starts to open afterwards.

subsequently propagated to the interior of the simulation sample. After the two wave fronts collide, they bounce off each other and travel to the opposite boundaries.

Fig. 9 shows a series of snapshots for the process. The three column corresponds to different time steps when the snapshots were taken ($n = 200$, $n = 300$, and $n = 450$). The first row shows the second component of the velocity field of the whole simulation sample, including both the atomistic region and continuum region. The values in the atomistic region were calculated by averaging over the atoms within each cell. In the first snapshot, the shock wave fronts parallel to the crack face propagate from the continuum boundary toward the centerline of the while simulation sample as in the second snapshot. After the two wave fronts reach the centerline, they behave differently behind and ahead of the crack tip. On the right half of the computational domain (ahead of the crack tip), the two wave fronts come across and cancel out each other, while on the left half of the domain (behind the crack tip), the two fronts hit the corresponding crack faces which play the role of free boundaries, and rebound to increase its own magnitude within the belonging region as in the third snapshot.

The second row shows the second components of displacements and of velocities along a vertical line that lies 3 macroscopic cells ahead of the original crack tip at the same time steps. The blue dots show values from the continuum finite volume scheme and the red dots show the average values from atomistic region. In the displacement plots, a dilative deformation with the shape of a slope propagates from the two ends towards the midpoint of the line, which correspond to two shock wave fronts of the velocity plots. In the first figure of this row, the left shock (velocity) travels from the left to the right and the right one travels from the right to the left. They came across each other in the second figure of this row. Up to this point, the displacement line was continuous, which means the corresponding atoms were close to each other

at that location. But in the last snapshot, a discontinuity is created, which implies that the crack tip has passed through this point.

The third (bottom) row shows the snapshots of the MD region at different time steps. The crack stayed still in the first two figure, but started to open in the third figure. This is caused by the two stress waves. In addition, one can see that the crack was brittle is in case.

We also tried different values k_I for the same type of loading condition. In particular, the crack opens when the magnitude of the stress reaches some threshold. Our simulations have shown that the lowest stress intensity factor k_I for which the crack opens is $k_I = 1.23k_I^c$, which is bigger than the value predicted by the Griffith criteria. In this sense, the Griffith criteria only works locally as a successful criteria.

5. Conclusions and further discussions

We have presented a multiscale method for coupling the molecular dynamics model and continuum elasto-dynamics under the HMM framework to study the dynamics of crystalline solids at zero temperature. The method is based on a domain decomposition idea. Away from local defects, the time evolution of the mechanical deformation is modeled by nonlinear elasto-dynamics, in which the standard Cauchy–Born rule is used to provide atomistic-based constitutive data. Near local defects, we refine the model to a full atomistic description. An interface condition is proposed to provide appropriate boundary conditions for the atomistic and continuum models so that the two time integration can alternate between the two regions.

The advantage of this approach is that it naturally decouples the time scales. However, several issues still remain. One issue is the thermal fluctuations. In this paper, we have only focused on the zero temperature case. At finite temperature, a similar interface condition can be derived [31]. In addition, energy flux can be computed at the interface to couple with the energy balance equation in the continuum model. However, the size of the time step at the interface, Δt , is usually too small to be able to filter out the noise in the fluxes. As a result, the solution of the continuum model will be quite noisy. These issues will be further studied in separate works.

There are a number of other issues that need to be addressed. The first is the issue of time steps. Although one main advantage of the formulation presented in [34] and adopted here is that it allows a natural treatment of the disparate macro and micro time scales, this has not been adequately explored. The problem is that near the crack, the continuum solution has a near singularity and therefore small spatial grids have to be used. In the current method, since we are using explicit finite volume methods, this dictates that we use small time steps. More general treatment of the continuum model is clearly needed.

The second related issue is the use of adaptive meshes in the continuum region. This is related to the problem discussed above: Since the solution in the continuum region is nearly singular near the crack tip – the singularity is regularized by the atomistic model, an adaptive strategy is clearly more advantageous.

Appendix A

A.1. Roe's scheme for elasto-dynamics model

Our basic macroscopic model is a set of conservation laws. We use Roe's linearization method as the macroscopic solver for the equation of conservation laws, see for example [20,29], for a complete description of the method. For convenience, we rewrite the conservation laws in the generic form,

$$\frac{\partial}{\partial t} \mathbf{w} + \nabla \cdot \mathbf{f}(\mathbf{w}) = 0, \quad (35)$$

where \mathbf{w} denotes the conserved quantities, and \mathbf{f} is some (unknown) flux function. In our elasto-dynamics problem, \mathbf{w} involves the deformation gradient and momentum, and \mathbf{f} contains the velocity and stress.

Denote the deformation gradient by $\varepsilon = \nabla \mathbf{u}$, then for 2D problems the variables in (35) involve the following components:

$$\mathbf{w} = \begin{pmatrix} \varepsilon_{11} \\ \varepsilon_{12} \\ \varepsilon_{21} \\ \varepsilon_{22} \\ \rho_0 v_1 \\ \rho_0 v_2 \\ \rho_0 e \end{pmatrix}, \quad \mathbf{f}_x = \begin{pmatrix} -v_1 \\ 0 \\ -v_2 \\ 0 \\ -\sigma_{11} \\ -\sigma_{21} \\ -v_1 \sigma_{11} - v_2 \sigma_{21} \end{pmatrix}, \quad \mathbf{f}_y = \begin{pmatrix} 0 \\ -v_1 \\ 0 \\ -v_2 \\ -\sigma_{21} \\ -\sigma_{22} \\ -v_1 \sigma_{21} - v_2 \sigma_{22} \end{pmatrix}, \quad (36)$$

where v_1 and v_2 are the two components of velocity.

The computational domain is partitioned into cells or volumes and we approximate the solution by piecewise constant, each of which is the average of the real solution over each cell. After integrating the equations over each cell and using the divergence theorem, we get

$$\frac{\mathbf{w}_i^{n+1} - \mathbf{w}_i^n}{\Delta t} + \sum_i F_{ij} \cdot \mathbf{n} = 0. \tag{37}$$

To compute the numerical fluxes F_{ij} we restrict the equations to the normal direction. We then arrive at a set of conservation laws in one dimension,

$$\partial_t \mathbf{w} + \partial_\eta \mathbf{f}(\mathbf{w}) = 0.$$

Since we are using piecewise constant construction, it is sufficient to solve the following problem, known as Riemann problem,

$$\begin{aligned} \partial_t \mathbf{w} + \partial_\eta \mathbf{f}(\mathbf{w}) &= 0, \\ \mathbf{w}(\eta, 0) &= \begin{cases} \mathbf{w}_L \eta < 0 \\ \mathbf{w}_R \eta > 0 \end{cases} \end{aligned}$$

and compute the flux at $\eta = 0$.

The key step of Roe’s method is to linearize the system around these two values. In particular, we look for a matrix $A(\mathbf{w}_L, \mathbf{w}_R)$ that satisfies

$$\mathbf{f}(\mathbf{w}_R) - \mathbf{f}(\mathbf{w}_L) = A(\mathbf{w}_R - \mathbf{w}_L), \quad A(\mathbf{w}, \mathbf{w}) = \nabla \mathbf{f}(\mathbf{w})$$

For instance for rectangular grid, along the x direction the Roe matrix can be constructed as follows,

$$A = - \begin{pmatrix} 0 & 0 & 0 & 0 & 1/\rho_0 & 0 \\ 0 & 0 & 0 & 0 & 0 & 0 \\ 0 & 0 & 0 & 0 & 0 & 1/\rho_0 \\ 0 & 0 & 0 & 0 & 0 & 0 \\ a_{51} & a_{52} & a_{53} & a_{54} & 0 & 0 \\ a_{61} & a_{62} & a_{63} & a_{64} & 0 & 0 \end{pmatrix}.$$

where

$$\left\{ \begin{aligned} a_{51} &= \frac{\sigma_{11}(e_{11}^R, e_{12}^R, e_{21}^R, e_{22}^R) - \sigma_{11}(e_{11}^L, e_{12}^L, e_{21}^L, e_{22}^L)}{e_{11}^R - e_{11}^L}, \\ a_{52} &= \frac{\sigma_{11}(e_{11}^L, e_{12}^R, e_{21}^R, e_{22}^R) - \sigma_{11}(e_{11}^L, e_{12}^L, e_{21}^L, e_{22}^L)}{e_{12}^R - e_{12}^L}, \\ a_{53} &= \frac{\sigma_{11}(e_{11}^L, e_{12}^L, e_{21}^R, e_{22}^R) - \sigma_{11}(e_{11}^L, e_{12}^L, e_{21}^L, e_{22}^L)}{e_{21}^R - e_{21}^L}, \\ a_{54} &= \frac{\sigma_{11}(e_{11}^L, e_{12}^L, e_{21}^L, e_{22}^R) - \sigma_{11}(e_{11}^L, e_{12}^L, e_{21}^L, e_{22}^L)}{e_{22}^R - e_{22}^L}, \\ a_{61} &= \frac{\sigma_{21}(e_{11}^R, e_{12}^R, e_{21}^R, e_{22}^R) - \sigma_{21}(e_{11}^L, e_{12}^L, e_{21}^L, e_{22}^L)}{e_{11}^R - e_{11}^L}, \\ a_{62} &= \frac{\sigma_{21}(e_{11}^L, e_{12}^R, e_{21}^R, e_{22}^R) - \sigma_{21}(e_{11}^L, e_{12}^L, e_{21}^L, e_{22}^L)}{e_{12}^R - e_{12}^L}, \\ a_{63} &= \frac{\sigma_{21}(e_{11}^L, e_{12}^L, e_{21}^R, e_{22}^R) - \sigma_{21}(e_{11}^L, e_{12}^L, e_{21}^L, e_{22}^L)}{e_{21}^R - e_{21}^L}, \\ a_{64} &= \frac{\sigma_{21}(e_{11}^L, e_{12}^L, e_{21}^L, e_{22}^R) - \sigma_{21}(e_{11}^L, e_{12}^L, e_{21}^L, e_{22}^L)}{e_{22}^R - e_{22}^L}, \end{aligned} \right.$$

Here $\sigma = \sigma(\boldsymbol{\varepsilon})$ is computed from the Cauchy–Born rule. If the denominator vanishes, the corresponding derivatives should be used, which is approximated by a divided difference formula.

Once A is obtained, we find its eigenvalues and eigenvectors,

$$A = U^{-1} \Lambda U, \quad U = [r_1, r_2, \dots, r_n].$$

For elasto-dynamics, the number of negative and positive eigenvalues are the same.

Now let $\mathbf{v} = U^{-1} \mathbf{w}$, we have

$$\partial_t \mathbf{v} + \Lambda \partial_\eta \mathbf{v} = 0.$$

This is a decoupled system of linear advection equations. If the eigenvalue is positive, the solution at $x = 0$ for $t > 0$ will be given by the left state, otherwise it will be given by the right state. Therefore,

$$\mathbf{f}(\mathbf{w}) = \mathbf{A}\mathbf{w} = \mathbf{f}(\mathbf{w}_L) + \sum \lambda_i^- (\mathbf{v}_R^i - \mathbf{v}_L^i) r_i \quad (38)$$

where i indicates the i th component and $-$ selects the negative part.

From the above description of the Roe's method as the macroscopic solver we can see that the only information we need from the microscopic model (atomistic model in the current case) is the fluxes at each grid point.

References

- [1] F.F. Abraham, J.Q. Broughton, N. Bernstein, E. Kaxiras, Spanning the continuum to quantum length scales in a dynamic simulation of brittle fracture, *Europhys. Lett.* 44 (6) (1998) 783–787.
- [2] S.A. Adelman, J.D. Doll, Generalized Langevin equation approach for atom/solid-surface scattering: Collinear atom/harmonic chain model, *J. Chem. Phys.* 61 (1974) 4242–4245.
- [3] M. Arndt, M. Griebel, Derivation of higher order gradient continuum models from atomistic models for crystalline solids, *SIAM Multiscale Model. Simul.* 4 (2005) 531–562.
- [4] N.W. Ashcroft, N.D. Mermin, *Solid State Physics*, Brooks Cole, 1976.
- [5] S. Badia, M. Parks, P. Bochev, M. Gunzburger, R. Lehoucq, On atomistic-to-continuum coupling by blending, *Multiscale Model. Simul.* 7 (1) (2008) 381–406.
- [6] T. Belytschko, S. Xiao, Coupling methods for continuum model with molecular model, *Int. J. Multiscale Comput. Eng.* 1 (2003) 1.
- [7] M. Born, K. Huang, *Dynamical Theory of Crystal Lattice*, Oxford University Press, 1954.
- [8] J.Q. Broughton, F.F. Abraham, N. Bernstein, E. Kaxiras, Concurrent coupling of length scales: methodology and application, *Phys. Rev. B* 60 (1999) 2391–2402.
- [9] W. Cai, M. de Koning, V.V. Bulatov, S. Yip, Minimizing boundary reflections in coupled-domain simulations, *Phys. Rev. Lett.* 85 (15) (2000) 3213–3216.
- [10] W. Chen, J. Fish, A generalized space-time mathematical homogenization theory for bridging atomistic and continuum scales, *Int. J. Numer. Mech. Eng.* 67 (2) (2006) 253–271.
- [11] K. Cheung, S. Yip, A molecular-dynamics simulation of crack-tip extension: the brittle-to-ductile transition, *Modell. Simul. Mater. Sci. Eng.* 2 (1994) 865–892.
- [12] M.S. Daw, M.I. Baskes, Embedded-atom method: derivation and application to impurities, surfaces, and other defects in metals, *Phys. Rev. B* 29 (12) (1984) 6443–6453.
- [13] W. E, B. Engquist, The heterogeneous multiscale methods, *Commun. Math. Sci.* 1 (2002) 87–132.
- [14] W. E, B. Engquist, X. Li, W. Ren, E. Vanden-Eijnden, Heterogeneous multiscale methods: a review, *Commun. Comput. Phys.* 2 (2007) 367–450.
- [15] W. E, Z. Huang, Matching conditions in atomistic-continuum modeling of materials, *Phys. Rev. Lett.* 87 (13) (2001) 135501.
- [16] W. E, Z. Huang, A dynamic atomistic-continuum method for the simulation of crystalline material, *J. Comput. Phys.* 182 (2002) 234–261.
- [17] W. E, X. Li, Multiscale modeling for crystalline solids, *Lecture Notes Comput. Sci. Eng.* 3 (2004) 3–22.
- [18] W. E, J. Lu, J.Z. Yang, Uniform accuracy of the quasicontinuum method, *Phys. Rev. B* 74 (2006) 214115.
- [19] W. E, P. Ming, Cauchy–Born rule and the stability of the crystalline solids: dynamic problems, *Acta Math. Appl. Sin. Engl. Ser.* 23 (2007) 529–550.
- [20] E. Godlewski, P.A. Raviart, *Numerical Approximation of Hyperbolic Systems of Conservation Laws*, Springer, 1996.
- [21] S. Godunov, A difference method for numerical calculation of discontinuous solutions of the equations of hydrodynamics, *Mater. Sb.* 47 (1959).
- [22] P. Gumbsch, S.J. Zhou, B.L. Holian, Molecular dynamics investigation of dynamic crack stability, *Phys. Rev. B* 55 (1997) 3445.
- [23] B.L. Holian, R. Ravelo, Fracture simulations using large-scale molecular dynamics, *Phys. Rev. B* 51 (17) (1995) 11275–11288.
- [24] J.H. Irving, J.G. Kirkwood, The statistical mechanical theory of transport processes iv, *J. Chem. Phys.* 18 (1950) 817–829.
- [25] E.G. Karpov, G.J. Wagner, W.K. Liu, A Green's function approach to deriving non-reflecting boundary conditions in molecular dynamics simulations, *Int. J. Numer. Meth. Eng.* 62 (9) (2005) 1250–1262.
- [26] J. Knap, M. Ortiz, An analysis of the quasicontinuum method, *J. Mech. Phys. Solids* 49 (2001) 1899–1923.
- [27] S. Kohlhoff, P. Gumbsch, H.F. Fischmeister, Crack propagation in b.c.c. crystals studied with a combined finite-element and atomistic model, *Phil. Mag.* A 64 (1991) 851–878.
- [28] R. LeSar, R. Najafabadi, D.J. Srolovitz, Finite-temperature defect properties from free energy minimization, *Phys. Rev. Lett.* 63 (1989) 624–627.
- [29] R.J. Leveque, *Numerical Methods for Conservation Laws*, Birkhauser, 2003.
- [30] X. Li, Variational boundary conditions for molecular dynamic in solids: treatment of the loading conditions, *J. Comput. Phys.* 227 (2008) 10078–10093.
- [31] X. Li, Boundary condition for molecular dynamics models for solids: a variational formulation based on lattice Green's functions, preprint.
- [32] X. Li, Efficient boundary condition for molecular statics models of solids, *Phys. Rev. B* 80 (2009) 104112.
- [33] X. Li, Stability of the boundary conditions for molecular dynamics, *J. Comput. Appl. Math.* 231 (2009) 493–505.
- [34] X. Li, W. E, Multiscale modeling of the dynamics of solids at finite temperature, *J. Mech. Phys. Solids* 53 (2005) 1650–1685.
- [35] X. Li, W. E, Variational boundary conditions for molecular dynamics simulations of solids at low temperature, *Commun. Comput. Phys.* 1 (2006) 136–176.
- [36] X. Li, W. E, Boundary conditions for molecular dynamics simulations of solids: treatment of the heat bath, *Phys. Rev. B* 76 (2007) 104107.
- [37] G. Lu, E. Kaxiras, Overview of multiscale simulations of materials, *Handbook of Theoretical and Computational Nanotechnology* (2005) 1–33.
- [38] A. Machova, G.J. Ackland, Dynamic overshoot in α -iron by atomistic simulations, *Modell. Simul. Mater. Sci. Eng.* 6 (1998) 521–542.
- [39] R.E. Miller, E.B. Tadmor, the Quasicontinuum method: overview, applications and current directions, *J. Computer-Aided Mater. Design* 9 (2002) 203–239.
- [40] R.E. Miller, E.B. Tadmor, A unified framework and performance benchmark of fourteen multiscale atomistic/continuum coupling methods, *Modell. Simul. Mater. Sci. Eng.* 17 (2009) 053001.
- [41] M. Mullins, M.A. Dokainish, Simulation of the (001) plane crack in α -iron employing a new boundary scheme, *Phil. Mag.* A 46 (1982) 771–787.
- [42] P.L. Roe, The use of the riemann problem in finite difference schemes, *Seventh Int. Conf. Numer. Methods Fluid Dyn.* 141 (1981) 354–359.
- [43] R.E. Rudd, J.Q. Broughton, Coarse-grained molecular dynamics and the atomic limit of finite element, *Phys. Rev. B* 58 (10) (1998) 5893–5896.
- [44] R.E. Rudd, J.Q. Broughton, Coarse-grained molecular dynamics: nonlinear finite elements and finite temperature, *Phys. Rev. B* 72 (2005) 144104.
- [45] V. Shastry, D. Farkas, Molecular statics simulation of crack propagation in α -Fe using EAM potentials, *Mater. Res. Soc. Symp. Proc.*, November 27–December 1, 1995, Boston, MA, United States, 1996, pp. 75–80.
- [46] V.B. Shenoy, R. Miller, E.B. Tadmor, R. Phillips, M. Ortiz, Quasicontinuum models of interfacial structure and deformation, *Phys. Rev. Lett.* 80 (4) (1998) 742–745.
- [47] V.B. Shenoy, R. Miller, E.B. Tadmor, D. Rodney, R. Phillips, M. Ortiz, An adaptive finite element approach to atomic-scale mechanics – the quasicontinuum method, *J. Mech. Phys. Solids* 47 (1999) 611–642.
- [48] L.E. Shilkrot, W.A. Curtin, R.E. Miller, A coupled atomistic/continuum model of defects in solids, *J. Mech. Phys. Solids* 50 (2002) 2085–2106.
- [49] L.E. Shilkrot, R.E. Miller, W.A. Curtin, Coupled atomistic and discrete dislocation plasticity, *Phys. Rev. Lett.* 89 (2002) 025501.
- [50] G. Sih, H. Liebowitz, *Fracture: An Advanced Treatise*, Academic, New York, 1968.

- [51] E.B. Tadmor, M. Ortiz, R. Phillips, Quasicontinuum analysis of defects in crystals, *Phil. Mag. A* 73 (1996) 1529–1563.
- [52] S. Tang, T.Y. Hou, W.K. Liu, A mathematical framework of the bridging scale method, *Int. J. Numer. Meth. Eng.* 65 (2006) 1688–1713.
- [53] S. Tang, T.Y. Hou, W.K. Liu, A pseudo-spectral multiscale method: interface conditions and coarse grid equations, *J. Comput. Phys.* 213 (2006) 57–85.
- [54] A.C. To, S. Li, Perfectly matched multiscale simulations, *Phys. Rev. B* 72 (2005) 035414.
- [55] G.J. Wagner, E.G. Karpov, W.K. Liu, Molecular dynamics boundary conditions for regular crystal lattice, *Comput. Method Appl. Mech. Eng.* 193 (2004) 1579–1601.
- [56] G.J. Wagner, W.K. Liu, Coupling of atomistic and continuum simulations using a bridging scale decomposition, *J. Comput. Phys.* 190 (2003) 249–274.
- [57] W. Wang, X. Li, C.W. Shu, The discontinuous Galerkin method for the multiscale modeling of dynamics of crystalline solids, *SIAM Multiscale Model. Simul.* 7 (2008) 294–320.
- [58] S.P. Xiao, T. Belytschko, A bridging domain method for coupling continua with molecular dynamics, *Comput. Methods Appl. Mech. Eng.* 193 (2004) 1645–1669.